1 **Title: DNA methylation regulates Vip3Aa resistance in fall armyworm (*Spodoptera frugiperda*)**

2 **Running title: DNA methylation mediates Vip3Aa resistance**

3

4 **Authors:** Luming Zou[1,†], Zhenxing Liu[1,†],Minghui Jin[1,†], Peng Wang[1], Yinxue Shan[1], Yutao Xiao[1]*

5 [1] Shenzhen Branch, Guangdong Laboratory of Lingnan Modern Agriculture, Key Laboratory of

6 Gene Editing Technologies (Hainan), Ministry of Agriculture and Rural Affairs, Agricultural

7 Genomics Institute at Shenzhen, Chinese Academy of Agricultural Sciences, Shenzhen, 518120, PR

8 China

9 [†] These authors contribute equally to this work.

10 *** Corresponding author**

11 Yutao Xiao, Email: xiaoyutao@caas.cn; Tel: +86-755-28473240

12 **Authors' e-mail addresses**

13 Luming Zou: lumingzou@hotmail.com

14 Zhenxing Liu: liuzhenxing@caas.cn

15 Minghui Jin: jinminghui@caas.cn

16 Peng Wang: wangpeng@caas.cn

17 Yinxue Shan: shanyinxue@caas.cn

18 **Abstract**

19 Vegetative insecticidal proteins (Vips) are widely used in pest management, but Vip resistance is a

20 big threat. DNA methylation plays important roles in regulating the response of biological

21 organisms to environmental stress. In this study, DNA methylation map was developed for fall

22 armyworm (FAW, *Spodoptera frugiperda*), and its function in regulating FAW Vip3Aa resistance

23 was explored. FAW was screened by Vip3Aa for 10 generations, and bioassays indicated that

24 Vip3Aa resistance increased trans-generationally. Based on the comparison of DNA methylation

25 maps between Vip3Aa-resistant and -susceptible strains showed that gene body methylation was

26 positively correlated with its expression. Moreover, the study demonstrated that a reduction in the

27 methylation density within the gene body of a 3'5'-cyclic nucleotide phosphodiesterase gene

28 resulted in decreased expression and increased resistance of FAW to Vip3Aa, which was validated

29 through RNAi experiments. The mechanism of Vip3Aa resistance will improve the understanding

30 of DNA methylation and its function in lepidoptera and provide a new perspective for making

31 strategies to pest management.

32 **Key words**: Vip3Aa resistance, DNA methylation, *Spodoptera frugiperda,* Adaptation

33
34

Introduction

The gram-positive bacterium *Bacillus thuringiensis* (Bt) is one of the most successful biopesticide in the last few decades, and transgenic crops that produce Bt toxins (Bt crop) have revolutionized pest control (Palma et al., 2014). The economic, environmental, and social benefits from Bt crops have deteriorated because of the rapid evolution of resistance (Xiao and Wu, 2019). The molecular mechanisms involved need to be determined to monitor, delay, and counter pest resistance. Vegetative insecticidal proteins (Vips), which are produced by Bt during its vegetative stages, have broad-spectrum activity against lepidopteran insects, and have no binding sites in common with any known Bt crystalline (Cry) proteins (Chakrabarty et al., 2020; Yang et al., 2021b). Fall armyworm (FAW), one of the most serious global invasive pests, has evolved Vip resistance (Bernardi et al., 2015; F. Yang et al., 2019; Yang et al., 2021a), and its resistance level has been increasing annually in the field (Yang et al., 2021a). However, the action of Vips insecticidal and genetic basis of resistant mechanism is still largely unknown (Chakrabarty et al., 2020).

DNA modification involves the transfer of a methyl group onto the C5 position of cytosine to form 5-methylcytosine (Moore et al., 2013). DNA methylation has a wide range of functions in regulating biological processes and the development of biological organisms by maintaining chromatin stability (Li et al., 2022), suppressing transposon activity (Jansz, 2019), and regulating gene expression mainly by managing transcriptional elements access (Zhang et al., 2018). Considering the plasticity and inheritability, DNA methylation is a main concern of adaptive mechanisms (Xu et al., 2020; Zhang et al., 2018). The characters of DNA methylation that regulate stress resistance are induced rapidly and inheritable (Kou et al., 2011; Verhoeven et al., 2010), but in some situations, the induced stress resistance is lost when stress is absent (Wibowo et al., 2016). DNA methylation regulates stress resistance in insects (Chen et al., 2020; Huang et al., 2019).

The potential for DNA methylation to regulate Bt resistance has received less attention. In the present study, the FAW obtained Vip3Aa tolerance generation by generation under Vip3Aa pressure, and it lost Vip3Aa tolerance gradually generation by generation when Vip3Aa pressure was released. Moreover, the FAW lab strain expressed DNA methylation diversity between individuals. Accordingly, a DNA methylation map was generated for the lab FAW strain by combining data from individuals. The DNA methylation maps were compared between susceptible and Vip3Aa

64 resistant strains. Our results indicated that DNA methylation play important roles in regulating FAW

65 Vip3Aa resistance.

Materials and methods

Insect rearing and resistance selection

68 The laboratory strain of *S. frugiperda* DH19 was obtained from DeHong (YunNan, China) and

69 established in January 2019. The strain was reared at 27±2 °C with 75%±10% relative humidity and

70 14:10 hours of light:dark photoperiod. The adults were supplied with 10% sucrose solution (Jin et

71 al., 2021). The DH19 strain was initially selected with 10 ppm Vip3Aa for five generations (F5) and

72 was continuously selected with 20 ppm Vip3Aa for five generations (F10).

Bioassays

74 The half-inhibition concentrations (IC_{50}) of Vip3Aa to FAW were determined by performing

75 bioassays. The Vip3Aa toxins used in this study were obtained from the Institute of Plant

76 Protection, Chinese Academy of Agricultural Sciences. The Vip3Aa surface overlay assays were

77 performed with neo-hatched larvae in 24-well tissue culture plates with surface area of 2 cm^2 for

78 each well. The Vip3Aa series concentration solutions were prepared by diluting Vip3Aa stock

79 solution into PBS (pH = 7.4). Gelatinous diet was transformed into the plate wells, and each well

80 was filled with 1 g of diet. After the diet solidified, 50 µL of Vip3Aa solution was added into each

81 well, and the final series concentrations are listed in Supplementary Table 1. The solutions were

82 spread evenly and dried in a fume hood. Each well was inoculated with one neonate, and each

83 concentration included 48 replicates. To avoid decay and Vip3Aa exhausting, the diet was renewed

84 after 84 h. After incubation for 7 days, each larva was weighted, and the IC_{50} was computed in

85 probit analysis.

Vip3Aa resistance inheritability tests

87 After selection with Vip3Aa for 10 generations, F10 expressed significantly 13-fold Vip3Aa

88 resistance compared with DH19. The inheritability of the Vip3Aa resistance for F10 was tested by

89 subjecting F10 to normal diet without Vip3Aa for three generations, and these generations were

90 subjected to bioassays.

Vip3Aa treatment and sampling

4

92 The effects of Vip3Aa treatment on FAW mid-guts transcriptomes and methylomes were

93 determined by treating the susceptible and resistant strains with Vip3Aa. For Vip3Aa treatment, the

94 neo-hatched larvae were fed by 10, 20, and 20 ppm Vip3Aa diet to fifth-instar, while the control

95 was fed with normal diet. The mid-guts of these larvae were dissected and washed with PBS (pH =

96 7.0) and flash frozen in liquid nitrogen. The mid-guts from 12 larvae were pooled to form a

97 biological replicate. The samples were stored at −80 °C before sequencing.

Processing of Oxford nanopore technique and RNA sequencing data

99 Oxford nanopore technique sequencing (ONT-Seq) and RNA sequencing (RNA-Seq) were

100 performed in Novogen (Beijing, China). The version 1.0 *S. frugiperda* reference genome

101 (GCF_011064685.1) was used for processing the sequencing data.

102 Megalodon (v2.3.3) was employed to process the nanopore raw data to extract methylation info. In

103 this process, Megalodon using guppy (v4.5.4) was used for base calling. The bed files produced

104 were used for subsequent analysis. Considering that the gene body mC densities were correlated

105 between replicates and were comparable between samples, and the mC densities were dependent on

106 sequencing depth, DESeq2 was employed to compare gene body mC numbers to identify DMGs. In

107 the process, mC numbers were normalized, thus eliminating bias, which was mediated by

108 sequencing depth. The RNA-Seq reads were mapped onto the reference genome by using Hisat2.

109 Then, the reads' coverage information was obtained and were passed to DESeq2 to identify DEGs.

RNA interference experiments

111 The primers for Sf*PDE8A* and *eGFP* were designed based on the reference sequences, and T7

112 promoter was added to the 5' end of the primers. All primers were synthesized by Sangon Biotech

113 (Shanghai, China; Supplementary Table 2). The total RNA was isolated from DH19 fifth-instar

114 larvae mid-guts sample by using TRIzol (Invitrogen, USA) according to the manufacturer's

115 protocol. Then, the extracted total RNA was reverse-transcribed into cDNA by using HiScript III 1st

116 Strand cDNA synthesis kit (Vazyme, China, Cat: R312). PCR was then performed with the cDNA

117 as template and the primers above to produce dsRNA templates. The dsRNA was synthesized with

118 T7 high-yield RNA transcription kit (Vazyme, China, Cat: TR101). The final dsRNA concentration

119 was adjusted to 2,500 ng/μL with water, and 100 nL of dsRNA was injected into the abdomen of the

120 third instar larvae of DH19 by using a glass capillary injection needle. A total of 120 larvae were

121 injected with dsRNAs targeting Sf*PDE8A* and *eGFP*. The larvae were kept on normal diet for 24 h,

122 and then transferred onto 20 ppm Vip3Aa diet. The larvae weight was recorded after 72 h to

123 estimate the growth inhibition rate. Then, the total RNA was extracted, and cDNA was synthesized

124 using HiScript III 1st Strand cDNA synthesis kit (Vazyme, China, Cat: R312) for quantitative real-

125 time PCR analysis. GAPDH was used as an internal control to normalize the gene expression level.

126 The primers used for qPCR are listed in supplementary Table 2.

Computation of normalized CpG contents and functional enrichment analysis

128 The normalized CpG contents [observed/expected (o/e)] were computed as $F_{CpG}/(F_C \times F_G)$. The

129 distribution profile of gene body CpG contents was predicted using mixtools (Benaglia et al., 2009).

130 The whole genome peptide sequences were annotated by eggNOG, and candidate gene sets were

131 enriched using ClusterProfiler (Yu et al., 2012).

Results

Vip3Aa resistance and inheritability during Vip3Aa screening

134 The bioassay of Vip3Aa on FAW revealed that the IC$_{50}$ of original generation (F0) was 6.23 ng/cm^2.

135 The IC$_{50}$ increased significantly to 13.67 ng/cm^2 ($P < 0.01$) and 81.73 ng/cm^2 ($P < 0.01$) after being

136 continuously screened for five (F5) and ten (F10) generations, respectively. The IC$_{50}$ value of F10

137 reached 13 times that of the wild type (Fig 1A). Vip3Aa susceptibility was gradually restored in the

138 following generations without Vip3Aa screening stress. After cultivation on normal diet for three

139 generations, the IC$_{50}$ value recovered to 15.08 ng/cm^2 (Fig 1B).

FAW mid-gut methylation map

141 The FAW mid-gut DNA methylation map was generated by ONT-seq on our lab strain. The ONT-

142 seq reads covered 98.24% of the reference genome. The mean coverage depth was 119 (mean =

143 118.43, median = 119; Supplementary Figure 1A). In the detected cytosines, 10.97% were

144 methylated. The mean methylation level was 1.19% (mean = 2.54%, median = 1.19%;

145 Supplementary Figure 1B). The methylcytosines (mC) were detected in CG, CHG, and CHH

146 contexts. In each of these contexts, 13.39, 1.60, and 4.11 million mCs were present (Supplementary

147 Figure 2) with proportions of 70.13%, 8.35%, and 21.52%, respectively (Fig 2A). For an overview

148 of the whole genomic methylation, the genome was divided into 50 kb end-to-end windows for

149 computing mC densities and mean methylation levels. The mC densities ranged from 0 to 0.033%.

150   The median and mean for the density values were 0.16% and 0.17%, respectively (Supplementary

151   Figure 1C). The 50 kb mean methylation levels ranged from 0.006% to 100%, and the mean and

152   median for the mean level values were 2.538% and 1.191%, respectively (Supplementary Figure

153   1D). The methylation status was also compared to correspondence genomic regional sequencing

154   coverage depth, normalized CpG contents, gene coding density, and gene expression levels. The

155   methylation status was highly correlated with sequencing depth. The mean methylation levels and

156   mC densities were negative and positively correlated with sequencing depth, respectively, whereas

157   the mean methylation levels were negatively correlated with mC densities. The methylation status

158   was not correlated with normalized CpG contents, gene coding densities, and gene expression levels

159   (Fig 2B, Supplementary Figure 3). *S. frugiperda* genomic regions expressed bimodal profile, but the

160   regional CpG contents did not express clear linear relationship with regional mC densities. *S.*

161   *frugiperda* genes also expressed a bimodal profile for their normalized CpG dinucleotide content

162   (Supplementary Figure 4A). Gene body mC densities were not correlated with their normalized

163   CpG contents (Supplementary Figure 4B). The methylated genes expressed similar mC density

164   patterns in the upstream, gene body, and downstream. While the majority of the methylated genes

165   exhibit a relatively low mC densities in their upstream regions, gene bodies, or downstream regions,

166   a subset of genes demonstrate an exceptionally high mC densities in one or more of these regions

167   (Fig 2C). The top 5% methylated genes for each stream had a small overlap (Supplementary Figure

168   5). GO enrichment analysis revealed that the top methylated genes were involved in house-keeping

169   processes, such as RNA processing, translation, and respiration (Supplementary Figure 6).

170   **DNA methylation conservation and variation during Vip3Aa screening**

171   Approximately 0.8–2 million mCs were detected in each sample. The mC numbers varied across

172   samples (Fig. 3A, Supplementary Figure 7A). The methylation levels expressed similar

173   distributions for each sample. The methylation levels clearly expressed two-peak patterns, a low

174   methylation level peak, and a high methylation level peak. The low-methylation-level (less than

175 30%) peak comprised the largest proportion of mC and the high-methylation-level (higher than

176 95%) peak comprised a small proportion of mC (Supplementary Figure 7B). The mC expressed

177 similar context proportions for each sample. The proportions of mC in CG, CHG, and CHH were

178 79.96%, 5.66%, and 14.39, respectively (Supplementary Figure 8).

179 Although Vip3Aa screening and treatment did not change the methylation level distributions, in F0

180 and F5, Vip3Aa treatment significantly decreased the number of mC ($P < 0.05$). In F10, where a

181 relatively high Vip3Aa resistance was observed, Vip3Aa treatment did not reduce the number of

182 mCs (Fig 3A). The mC levels and sites were less correlated between any of the two samples

183 (Supplementary Figure 9). In many studies, differentially methylated regions (DMR) were

184 identified in the range of 100–500 bp (Herb et al., 2012; Rajkumar et al., 2020). To evaluate the

185 conservation of methylation in 500 bp region between samples, the mC density and mean

186 methylation levels in 500 bp window slipping by 100 bp steps on the genome were computed and

187 their pairwise correlation were detected. The results indicated that 500 bp window methyl cytosine

188 densities and mean methylation levels were also less correlated for any two samples

189 (Supplementary Figure 10). Since gene expression could be regulated by gene region mC s.

190 Upstream, gene body, and downstream mC densities and mean methylation levels were computed.

191 The pairwise correlation analysis of the gene region mC densities and mean methylation levels

192 revealed that the mC densities were highly correlated in the upstream, gene body, and downstream,

193 whereas the mean methylation levels were not (Supplementary Figure 11). The methylated genes

194 expressed similar mC density patterns in the upstream, gene body, and downstream (Supplementary

195 Figure 12).

196 Principle components analysis (PCA) on each gene stream mC density of each samples revealed

197 that the F10 samples were clearly isolated from other samples. The F10 control group and Vip3Aa

198 treatment group could not be distinguished. In F0 and F5, the samples could neither be demarcated

199 by generations nor treatment (Figs 3B, C, D). Considering that the F10 samples were demarcated by

200 PCA, differentially methylated genes (DMG) were identified by comparing F10 to F5 and F10 to F0

201 on each gene stream mC densities. Approximately 135, 370, and 116 DMGs were identified in the

202 upstream, gene body, and downstream regions, respectively (Supplementary Figures 13A, B, C).

203 The DMG for each stream had a small overlap (Supplementary Figure 13D). The DMG clearly

204 expressed two-cluster mC density patterns (Fig 4). The first cluster DMG expressed high mC

205 density in the F0 and F5 samples, while the second cluster DMG expressed high mC density in the

206 F10 samples. The SD values of DMGs was also computed from the three replicates. The genes that

207 express high mC densities in F10 also expressed high SD values and vice versa.

Differentially expressed genes based on Vip3Aa screening

209 PCA on gene *tags* per kilobase *per million mapped reads* (TPM) values for each sample revealed

210 that F10- and Vip3Aa-treated F10 samples were distinguished from the other samples. However,

211 F10- and Vip3Aa-treated samples cannot be distinguished. Vip3Aa-treated F0 and F5 samples were

212 clearly demarcated from the other samples on the second and first PC level, respectively. F0 and F5

213 control samples could not be distinguished from their treatment samples (Supplementary Figure

214 14A). Based on the mC PCA, the tenth-generation samples were distinguished from the other

215 samples. Comparison was carried out between the tenth- and fifth-generation and between the tenth-

216 generation and wild-type samples to identify differentially expressed genes (DEGs). Finally, 2,850

217 DEGs were identified (Supplementary Figure 14B). The DEGs clearly expressed two-cluster

218 expression patterns. The first cluster of genes expressed high expression levels in the tenth

219 generation. The second cluster of genes expressed low expression levels in the tenth generation

220 compared with F0 and F5 (Supplementary Figure 15). Two and four KEGG pathways were

221 significantly enriched ($P_{fdr} < 0.05$) in the first and second cluster, respectively. P450 was

222 significantly enriched and had the highest enrichment ratio in the second cluster (Figure 5A). A total

223 of 12 P450 genes were differentially expressed, in which nine genes were methylated in the

224 upstream or gene body. However, only one of these nine P450 genes were differentially methylated

9

225   in its gene body (Figure 5B). These P450 genes expressed higher expression levels in the F10- and

226   Vip3Aa-treated F10. Their expression levels were not correlated with their methylation densities,

227   except for the differentially methylated one (XM_035588305.1, Figure 5C, Supplementary Figure

228   16).

Relationship between DMGs and DEGs

230   A total of 199 DEGs were differentially methylated in their upstream or downstream. The largest

231   proportion (72.4%) of these genes were differentially methylated at their gene body. A total of 54

232   DEGs were differentially methylated at their upstream. However, 26 of these genes were

233   differentially methylated at their gene body or downstream. More than half of the downstream

234   differentially methylated DEGs were also differentially methylated at their gene body

235   (Supplementary Figure 17). The effects of DNA methylation on gene expression were determined

236   by performing linear relationship analysis of the fold change of expression level and mC densities

237   for each stream between F10 and F0 and between F10 and F5. The gene body and downstream

238   differentially methylated genes expressed clear linear relationship between the fold change of

239   expression level and mC density. However, the fold change of expression level and upstream mC

240   density had a low linear relationship (Figure 6, Supplementary Figure 18, Supplementary Figure

241   19).

SfPDE8A gene contribute to Vip3Aa resistance

243   The gene LOC118265840 expressed extremely high methylation density in the F10- and Vip3Aa-

244   treated F10. The gene was differentially expressed and methylated (Figure 6). Based on functional

245   annotation, the gene was identified as the SfPDE8A gene, which belongs to PDE8 subfamily. Two

246   SfPDE8 genes were identified in the FAW genome, and both genes were located on the seventh

247   chromosome (NC_049717.1). These genes were nominated as *SfPDE8A* (LOC118265840) and

248   *SfPDE8B* (LOC118265759) according to their location. In F0, Vip3Aa treatment significantly

249   increased *SfPDE8A* expression level and methylation density ($P < 0.05$). In F5, Vip3Aa

250 significantly reduced *SfPDE8A* expression level and methylation density ($P < 0.05$). However, in

251 F10, the expression level of *SfPDE8A* and methylation density were not altered by Vip3Aa

252 treatment (Figure 7A, B, C). qPCR result indicated that the *SfPDE8A* expression level was

253 significantly reduced to a half by RNAi ($P < 0.05$, Figure 8A). The RNAi of this gene significantly

254 increased the FAW growth rate when fed with Vip3Aa diet ($P < 0.05$; Figure 8B).

Discussion

FAW rapidly obtained Vip3Aa resistance

257 Organisms acquire long-term and short-term resistance to biotic and abiotic stresses through

258 different mechanisms. Genetic variations contribute to long-term evolved stress resistance

259 (Prodhomme et al., 2020), while epigenetic modifications contribute to short-term obtained stress

260 resistance (Dowen et al., 2012; Stassen et al., 2018). Epigenetic modification determined stress

261 resistances that are inheritable in few generations, which are lost in the long run (Boyko et al.,

262 2010). Long time Bt stress lead to mutations on Bt toxin resistance correlated genes, which lead to

263 permanent Bt resistance resistance in Lepidoptera insects (X. Yang et al., 2019). In the present

264 study, FAW obtained inheritable Vip3Aa resistance in several generations under Vip3Aa pressure.

265 The Vip3Aa resistance increased with the Vip3Aa screened generation numbers. Its Vip3Aa

266 resistance gradually decreased after Vip3Aa stress was eliminated. Therefore, Vip3Aa resistance

267 can be regulated by epigenetic modification. DNA methylation modification is an epigenetic change

268 that contributes to stress resistance (Ding et al., 2022; Sun et al., 2021). Accordingly, the effects of

269 DNA methylation variation on Vip3Aa resistance was studied in FAW.

Characteristics of FAW DNA methylation map

271 The DNA methylation map varies across tissues in a specific biological organism (Marshall et al.,

272 2019; Rajkumar et al., 2020; Zhang et al., 2013). DNA methylation maps are highly conserved in a

273 specific tissue between individuals within a species (Uli et al., 2018; Wang et al., 2021). However,

274 in the present study, the FAW mid-gut methylation status was less conserved in our laboratory strain

11

275   individuals at the single nucleotide level compared with that in previous studies. All the sequencing

276   results were combined to generate a methylation map for the laboratory FAW strain DH-19.

277   In our FAW DNA methylation map, the mCs were detected in CG, CHG, and CHH (H represents A,

278   T, or G) contexts. The DNA methyltransferases 3 (DNMT3) catalyzes non-CG context methylation,

279   but DNMT3 is lost in Lepidoptera, and CHH context methylation is not observed in Lepidoptera

280   (Glastad et al., 2011; Omar et al., 2020).

281   However, CHH methylation was identified in *Bombyx mori* (Lepidoptera:Bombycidae), albeit in an

282   extremely small proportion (Li et al., 2020), and in the absence of DNMT3 *(Gao et al., 2020)*. The

283   whole FAW reference genome was scanned, but no DNMT3 was identified and more than 20% mC

284   was in CHH context. Therefore, a novel and distinct pathway can be determined for non-CG

285   methylation in FAW.

286   Considering that the methylation status is less conserved between individuals, the methylation

287   levels are negatively correlated with sequencing depth, and the mC densities are positively

288   correlated with the sequencing depth. The less conservation also resulted in low methylation levels.

289   In this strain methylation map, the proportion of mC in CG was smaller than that in separated

290   samples, while the proportions of mC in CHG and CHH were larger than those in separated

291   samples. Therefore, the methylation status is more highly conserved in CG context than in CHG

292   and CHH contexts in FAW.

293   Gene body CpG dinucleotide contents are considered to be a proxy for DNA methylation, which is

294   negatively correlated with normalized CpG contents in *Apis mellifera* (Glastad et al., 2011). The

295   normalized CpG contents of *S. frugiperda* gene body expressed a bimodal profile that is similar to

296   that in *Bombyx mori*. However, gene body mC densities were not correlated with normalized CpG

297   contents. Gene bodies are preferentially methylated in insects (Wang et al., 2013; Xu et al., 2021;

298   Zemach et al., 2010). However, in the present study, FAW DNA methylation was evenly distributed

299 alongside the genome. The DNA methylation features might contribute to FAW-specific migration

300 and invasive characteristics. In the present study, although the genes expressed similar mC densities

301 in their either streams, extremely high-density methylated genes were still observed. GO enrichment

302 indicated that these genes were enriched in house-keeping pathways (Supplementary Figure 6).

303 These results are consistent with the findings in arthropods (Lewis et al., 2020).

304 **FAW methylation variation resulted by Vip3Aa screening**

305 DNA methylation is maintained with high fidelity under stress (Sun et al., 2021; Wang et al., 2015).

306 The results of the present study indicate that methylation level distributions and methylated context

307 proportions remained unchanged transgenerationally under Vip3Aa screening in FAW. In potato

308 beetle (*Leptinotarsa decemlineata*), mC counts decreased because of pesticide treatment (Brevik et

309 al., 2021). In the present study, in F0, Vip3Aa treatment significantly reduced the mC counts.

310 However, in F5 and F10, where significant Vip3Aa resistance was expressed, Vip3Aa treatment did

311 not reduce the mC counts.

312 Genomic methylation variations have been observed transgenerationally under stress (Stassen et al.,

313 2018). In the present study, genomic DNA methylation variation was observed between Vip3Aa

314 screened generation and original generation. In many studies, DMRs are identified up to 500 bp

315 regions on the genome (Herb et al., 2012; Rajkumar et al., 2020). However, in the present study,

316 DNA methylation was not conserved at the single-nucleotide level between samples. The

317 methylation status was not conserved at the 500-bp level. Hence, the methylation was not

318 comparable between the sample at single nucleotide level nor at the 500-bp level. The results

319 indicate that the gene region mC densities were highly conserved between samples, and mC

320 densities were positively correlated with sequencing depth, which varied across replicates. The mC

321 densities of each gene region were normalized and compared to identify DMGs.

322 Some of the DMG expressed positive correlation between mC density and SD values. Considering

323 that the mC density of these genes were correlated with Vip3Aa resistance, the mC densities were

324 under selection during Vip3Aa screening.

Gene body DNA methylation was positively correlated with gene expression

326 Genic regions are preferentially methylated in insects (Glastad et al., 2011). The DNA methylation

327 map of FAW established in the present study is not consistent with this conclusion. The current

328 results indicate that mC is distributed evenly on the genome. DNA methylation regulates gene

329 expression mainly by regulating transcription element access. Upstream DNA methylation always

330 represses gene expression by directly inhibiting the binding of transcriptional factors (Zhang et al.,

331 2018). The relationship between gene body DNA methylation and gene expression is unclear from

332 the studies in vertebrates and plants. Gene body methylation promotes gene expression (Yang et al.,

333 2014), whereas some studies have obtained opposite findings (Jjingo et al., 2012; Zou et al., 2020).

334 Gene body methylation is positively correlated with gene expression in insects (Li et al., 2020; Xu

335 et al., 2021). In the present study, gene body and downstream mC density variation expressed

336 clearly linear relationships with gene expression level variation. The upstream mC density variation

337 was also positively correlated with the gene expression level variation, but the correlation was not

338 significantly correlated ($P < 0.05$). This finding was obtained possibly because more than half of the

339 genes had differentially methylated upstream accompanied with different methylation in their gene

340 bodies. The expression levels of these genes were simultaneously affected by their upstream and

341 gene body methylation, thus causing these results. More than half of the genes had differentially

342 methylated downstream accompanied with different methylation in their gene bodies. These results

343 indicate that gene body mC density variation is positively correlated with the gene expression level.

344 However, the effect of downstream DNA methylation on gene expression has not been determined.

cAMP pathway was involved in FAW Vip3Aa resistance

346 Cyclic adenosine monophosphate (cAMP) is a secondary messenger that is involved in the

347 regulation many metabolic pathways and biological processes (Shaw et al., 2022). In insects, it

348 regulates the expression of P450 genes (Li and Liu, 2017; Watanabe et al., 2017), which contribute

349 to numerous xenobiotics resistance (Lu et al., 2021). The upregulation of P450 genes might increase

350 FAW Bt resistance (Boaventura et al., 2021). cAMP-phosphodiesterase (PDE) catalyzes cAMP

351 hydrolysis and inhibits cAMP signal transduction pathway (Bender and Beavo, 2006; Houslay,

352 2010). In the present study, the *SfPDE8A* gene expressed gene body demethylation in Vip3Aa

353 screened FAW, which expressed significant Vip3Aa resistance. Some P450 genes were upregulated

354 in the Vip3Aa screened FAW. The knockdown of *SfPDE8A* significantly increased FAW Vip3Aa

355 resistance. Therefore, FAW increased its Vip3Aa resistance via the cAMP pathway.

Conclusions

357 Under Vip3Aa pressure, FAW acquired Vip3Aa resistance, which was regulated by DNA
358 methylation variation. At the single nucleotide level, our laboratory strain expressed DNA
359 methylation diversity in their mid-gut. The FAW DNA methylation status was under selection
360 during Vip3Aa screening. In FAW, gene body mC densities were positively correlated with gene
361 expression levels. Demethylation in the gene body of *SfPDE8A* gene decreased its expression,
362 which might increase P450 gene expression via the cAMP signal pathway and increased FAW
363 Vip3Aa resistance.

364

365 Benaglia T, Chauveau D, Hunter DR, Young D. 2009. mixtools: An R Package for Analyzing Finite
366   Mixture Models. *Journal of Statistical Software* **32**:1–29.
367 Bender AT, Beavo JA. 2006. Cyclic Nucleotide Phosphodiesterases: Molecular Regulation to
368   Clinical Use. *Pharmacological Reviews* **58**:488–520. doi:10.1124/PR.58.3.5
369 Bernardi O, Bernardi D, Ribeiro RS, Okuma DM, Salmeron E, Fatoretto J, Medeiros FCL, Burd T,
370   Omoto C. 2015. Frequency of resistance to Vip3Aa20 toxin from Bacillus thuringiensis in
371   Spodoptera frugiperda (Lepidoptera: Noctuidae) populations in Brazil. *Crop Protection*
372   **76**:7–14. doi:10.1016/j.cropro.2015.06.006
373 Boaventura D, Buer B, Hamaekers N, Maiwald F, Nauen R. 2021. Toxicological and molecular
374   profiling of insecticide resistance in a Brazilian strain of fall armyworm resistant to Bt Cry1
375   proteins. *Pest Management Science* **77**:3713–3726. doi:10.1002/ps.6061
376 Boyko A, Blevins T, Yao Y, Golubov A, Bilichak A, Ilnytskyy Y, Hollander J, Meins F, Kovalchuk I.
377   2010. Transgenerational adaptation of Arabidopsis to stress requires DNA methylation and
378   the function of dicer-like proteins. *PLoS ONE* **5**. doi:10.1371/journal.pone.0009514
379 Brevik K, Bueno EM, McKay S, Schoville SD, Chen YH. 2021. Insecticide exposure affects
380   intergenerational patterns of DNA methylation in the Colorado potato beetle, Leptinotarsa
381   decemlineata. *Evolutionary Applications* **14**:746–757. doi:10.1111/eva.13153
382 Chakrabarty S, Jin M, Wu C, Chakraborty P, Xiao Y. 2020. Bacillus thuringiensis vegetative
383   insecticidal protein family Vip3A and mode of action against pest Lepidoptera. *Pest*
384   *Management Science* **76**:1612–1617. doi:10.1002/ps.5804
385 Chen P, Xiao WF, Pan MH, Xiao JS, Feng YJ, Dong ZQ, Zou BX, Zhou L, Zhang YH, Lu C. 2020.
386   Comparative genome-wide DNA methylation analysis reveals epigenomic differences in
387   response to heat-humidity stress in Bombyx mori. *International Journal of Biological*
388   *Macromolecules* **164**:3771–3779. doi:10.1016/j.ijbiomac.2020.08.251
389 Ding G, Cao L, Zhou J, Li Z, Lai Y, Liu K, Luo Y, Bai L, Wang X, Wang T, Wang R, Yang G, Sun
390   S. 2022. DNA Methylation Correlates with the Expression of Drought-Responsive Genes
391   and Drought Resistance in Rice. *Agronomy* **12**:1445. doi:10.3390/agronomy12061445
392 Dowen RH, Pelizzola M, Schmitz RJ, Lister R, Dowen JM, Nery JR, Dixon JE, Ecker JR. 2012.
393   Widespread dynamic DNA methylation in response to biotic stress. *Proceedings of the*
394   *National Academy of Sciences of the United States of America* **109**.
395   doi:10.1073/pnas.1209329109
396 Gao R, Li C-L, Tong X-L, Han M-J, Lu K-P, Liang S-B, Hu H, Luan Y, Zhang B-L, Liu Y-Y, Dai F-
397   Y. 2020. Identification, expression, and artificial selection of silkworm epigenetic
398   modification enzymes. *BMC Genomics* **21**:740. doi:10.1186/s12864-020-07155-z
399 Glastad KM, Hunt BG, Yi SV, Goodisman MAD. 2011. DNA methylation in insects: On the brink
400   of the epigenomic era. *Insect Molecular Biology* **20**:553–565. doi:10.1111/j.1365-
401   2583.2011.01092.x
402 Herb BR, Wolschin F, Hansen KD, Aryee MJ, Langmead B, Irizarry R, Amdam GV, Feinberg AP.
403   2012. Reversible switching between epigenetic states in honeybee behavioral subcastes. *Nat*
404   *Neurosci* **15**:1371–1373. doi:10.1038/nn.3218
405 Huang H, Wu P, Zhang S, Shang Q, Yin H, Hou Q, Zhong J, Guo X. 2019. DNA methylomes and
406   transcriptomes analysis reveal implication of host DNA methylation machinery in BmNPV
407   proliferation in Bombyx mori. *BMC Genomics* **20**. doi:10.1186/s12864-019-6146-7
408 Jansz N. 2019. DNA methylation dynamics at transposable elements in mammals. *Essays in*
409   *Biochemistry* **63**:677–689. doi:10.1042/EBC20190039
410 Jin M, Tao J, Li Q, Cheng Y, Sun X, Wu K, Xiao Y. 2021. Genome editing of the SfABCC2 gene
411   confers resistance to Cry1F toxin from Bacillus thuringiensis in Spodoptera frugiperda.
412   *Journal of Integrative Agriculture* **20**:815–820. doi:10.1016/S2095-3119(19)62772-3
413 Jjingo D, Conley AB, Yi SV, Lunyak VV, Jordan IK. 2012. On the presence and role of human
414   gene-body DNA methylation. *Oncotarget* **3**:462–474. doi:10.18632/oncotarget.497

415 Kou HP, Li Y, Song XX, Ou XF, Xing SC, Ma J, Von Wettstein D, Liu B. 2011. Heritable alteration
416   in DNA methylation induced by nitrogen-deficiency stress accompanies enhanced tolerance
417   by progenies to the stress in rice (Oryza sativa L.). *Journal of Plant Physiology* **168**:1685–
418   1693. doi:10.1016/j.jplph.2011.03.017
419 Lewis SH, Ross L, Bain SA, Pahita E, Smith SA, Cordaux R, Miska EA, Lenhard B, Jiggins FM,
420   Sarkies P. 2020. Widespread conservation and lineage-specific diversification of genome-
421   wide DNA methylation patterns across arthropods. *PLoS Genetics* **16**.
422   doi:10.1371/journal.pgen.1008864
423 Li B, Hu P, Zhu L-B, You L-L, Cao H-H, Wang J, Zhang S-Z, Liu M-H, Toufeeq S, Huang S-J, Xu
424   J-P. 2020. DNA Methylation Is Correlated with Gene Expression during Diapause
425   Termination of Early Embryonic Development in the Silkworm (Bombyx mori).
426   *International Journal of Molecular Sciences* **21**:671. doi:10.3390/ijms21020671
427 Li S, Peng Y, Panchenko AR. 2022. DNA methylation: Precise modulation of chromatin structure
428   and dynamics. *Current Opinion in Structural Biology* **75**:102430.
429   doi:10.1016/j.sbi.2022.102430
430 Li T, Liu N. 2017. Regulation of P450-mediated permethrin resistance in Culex quinquefasciatus by
431   the GPCR/Gαs/AC/cAMP/PKA signaling cascade. *Biochemistry and Biophysics Reports*
432   **12**:12–19. doi:10.1016/j.bbrep.2017.08.010
433 Lu K, Song Y, Zeng R. 2021. The role of cytochrome P450-mediated detoxification in insect
434   adaptation to xenobiotics. *Current Opinion in Insect Science* **43**:103–107.
435   doi:10.1016/j.cois.2020.11.004
436 Marshall H, Lonsdale ZN, Mallon EB. 2019. Methylation and gene expression differences between
437   reproductive and sterile bumblebee workers. *Evolution Letters* **3**:485–499.
438   doi:10.1002/evl3.129
439 Moore LD, Le T, Fan G. 2013. DNA methylation and its basic function.
440   *Neuropsychopharmacology: Official Publication of the American College of*
441   *Neuropsychopharmacology* **38**:23–38. doi:10.1038/npp.2012.112
442 Omar MAA, Li M, Liu F, He K, Qasim M, Xiao H, Jiang M, Li F. 2020. The Roles of DNA
443   Methyltransferases 1 (DNMT1) in Regulating Sexual Dimorphism in the Cotton Mealybug,
444   Phenacoccus solenopsis. *Insects* **11**:121. doi:10.3390/insects11020121
445 Palma L, Muñoz D, Berry C, Murillo J, Caballero P, Caballero P. 2014. Bacillus thuringiensis
446   toxins: An overview of their biocidal activity. *Toxins* **6**:3296–3325.
447   doi:10.3390/toxins6123296
448 Prodhomme C, Vos PG, Paulo MJ, Tammes JE, Visser RGF, Vossen JH, van Eck HJ. 2020.
449   Distribution of P1(D1) wart disease resistance in potato germplasm and GWAS
450   identification of haplotype-specific SNP markers. *Theoretical and Applied Genetics*
451   **133**:1859–1871. doi:10.1007/s00122-020-03559-3
452 Rajkumar MS, Gupta K, Khemka NK, Garg R, Jain M. 2020. DNA methylation reprogramming
453   during seed development and its functional relevance in seed size/weight determination in
454   chickpea. *Communications Biology* **3**. doi:10.1038/s42003-020-1059-1
455 Shaw S, Knüsel S, Abbühl D, Naguleswaran A, Etzensperger R, Benninger M, Roditi I. 2022.
456   Cyclic AMP signalling and glucose metabolism mediate pH taxis by African trypanosomes.
457   *Nature Communications* **13**:1–13. doi:10.1038/s41467-022-28293-w
458 Stassen JHM, López A, Jain R, Pascual-Pardo D, Luna E, Smith LM, Ton J. 2018. The relationship
459   between transgenerational acquired resistance and global DNA methylation in Arabidopsis.
460   *Scientific Reports* **8**. doi:10.1038/s41598-018-32448-5
461 Sun R-Z, Liu J, Wang Y-Y, Deng X. 2021. DNA methylation-mediated modulation of rapid
462   desiccation tolerance acquisition and dehydration stress memory in the resurrection plant
463   Boea hygrometrica. *PLOS Genetics* **17**:e1009549. doi:10.1371/journal.pgen.1009549

Uli N, Michelen-Gomez E, Ramos EI, Druley TE. 2018. Age-specific changes in genome-wide methylation enrich for Foxa2 and estrogen receptor alpha binding sites. *PLOS ONE* **13**:e0203147. doi:10.1371/journal.pone.0203147

Verhoeven KJF, Jansen JJ, van Dijk PJ, Biere A. 2010. Stress-induced DNA methylation changes and their heritability in asexual dandelions. *New Phytologist* **185**:1108–1118. doi:10.1111/j.1469-8137.2009.03121.x

Wang W, Huang F, Qin Q, Zhao X, Li Z, Fu B. 2015. Comparative analysis of DNA methylation changes in two rice genotypes under salt stress and subsequent recovery. *Biochemical and Biophysical Research Communications* **465**:790–796. doi:10.1016/j.bbrc.2015.08.089

Wang X, Li A, Wang W, Que H, Zhang G, Li L. 2021. DNA methylation mediates differentiation in thermal responses of Pacific oyster (Crassostrea gigas) derived from different tidal levels. *Heredity* **126**:10–22. doi:10.1038/s41437-020-0351-7

Wang X, Wheeler D, Avery A, Rago A, Choi J-H, Colbourne JK, Clark AG, Werren JH. 2013. Function and Evolution of DNA Methylation in Nasonia vitripennis. *PLOS Genetics* **9**:e1003872. doi:10.1371/journal.pgen.1003872

Watanabe H, Sugimoto R, Ikegami K, Enoki Y, Imafuku T, Fujimura R, Bi J, Nishida K, Sakaguchi Y, Murata M, Maeda H, Hirata K, Jingami S, Ishima Y, Tanaka M, Matsushita K, Komaba H, Fukagawa M, Otagiri M, Maruyama T. 2017. Parathyroid hormone contributes to the down-regulation of cytochrome P450 3A through the cAMP/PI3K/PKC/PKA/NF-κB signaling pathway in secondary hyperparathyroidism. *Biochemical Pharmacology* **145**:192–201. doi:10.1016/j.bcp.2017.08.016

Wibowo A, Becker C, Marconi G, Durr J, Price J, Hagmann J, Papareddy R, Putra H, Kageyama J, Becker J, Weigel D, Gutierrez-Marcos J. 2016. Hyperosmotic stress memory in Arabidopsis is mediated by distinct epigenetically labile sites in the genome and is restricted in the male germline by DNA glycosylase activity. *Elife* **5**:e13546. doi:10.7554/eLife.13546

Xiao Y, Wu K. 2019. Recent progress on the interaction between insects and Bacillus thuringiensis crops. *Philosophical Transactions of the Royal Society B: Biological Sciences* **374**. doi:10.1098/rstb.2018.0316

Xu G, Lyu H, Yi Y, Peng Y, Feng Q, Song Q, Gong C, Peng X, Palli SR, Zheng S. 2021. Intragenic DNA methylation regulates insect gene expression and reproduction through the MBD/Tip60 complex. *iScience* **24**:102040. doi:10.1016/j.isci.2021.102040

Xu G, Lyu J, Li Q, Liu H, Wang D, Zhang M, Springer NM, Ross-Ibarra J, Yang J. 2020. Evolutionary and functional genomics of DNA methylation in maize domestication and improvement. *Nature Communications* **11**. doi:10.1038/s41467-020-19333-4

Yang F, Kerns DL, Little NS, Santiago González JC, Tabashnik BE. 2021a. Early Warning of Resistance to Bt Toxin Vip3Aa in Helicoverpa zea. *Toxins (Basel)* **13**:618. doi:10.3390/toxins13090618

Yang F, Williams J, Huang F, Kerns DL. 2021b. Genetic basis and cross-resistance of Vip3Aa resistance in Spodoptera frugiperda (lepidoptera: Noctuidae) derived from Texas, USA. *Crop Protection* **147**:105702. doi:10.1016/j.cropro.2021.105702

Yang F, Williams J, Porter P, Huang F, Kerns DL. 2019. F2 screen for resistance to Bacillus thuringiensis Vip3Aa51 protein in field populations of Spodoptera frugiperda (Lepidoptera: Noctuidae) from Texas, USA. *Crop Protection* **126**:104915. doi:10.1016/j.cropro.2019.104915

Yang X, Chen W, Song X, Ma X, Cotto-Rivera RO, Kain W, Chu H, Chen YR, Fei Z, Wang P. 2019. Mutation of ABC transporter ABCA2 confers resistance to Bt toxin Cry2Ab in Trichoplusia ni. *Insect Biochemistry and Molecular Biology* **112**:103209. doi:10.1016/j.ibmb.2019.103209

512 Yang X, Han H, DeCarvalho DD, Lay FD, Jones PA, Liang G. 2014. Gene body methylation can
513   alter gene expression and is a therapeutic target in cancer. *Cancer Cell* **26**:577–590.
514   doi:10.1016/j.ccr.2014.07.028
515 Yu G, Wang LG, Han Y, He QY. 2012. ClusterProfiler: An R package for comparing biological
516   themes among gene clusters. *OMICS A Journal of Integrative Biology* **16**:284–287.
517   doi:10.1089/omi.2011.0118
518 Zemach A, McDaniel IE, Silva P, Zilberman D. 2010. Genome-wide evolutionary analysis of
519   eukaryotic DNA methylation. *Science* **328**:916–919. doi:10.1126/science.1186366
520 Zhang Bo, Zhou Y, Lin N, Lowdon RF, Hong C, Nagarajan RP, Cheng JB, Li D, Stevens M, Lee
521   HJ, Xing X, Zhou J, Sundaram V, Elliott G, Gu J, Shi T, Gascard P, Sigaroudinia M, Tlsty
522   TD, Kadlecek T, Weiss A, O'Geen H, Farnham PJ, Maire CL, Ligon KL, Madden PAF, Tam
523   A, Moore R, Hirst M, Marra MA, Zhang Baoxue, Costello JF, Wang T. 2013. Functional
524   DNA methylation differences between tissues, cell types, and across individuals discovered
525   using the M&M algorithm. *Genome Res* **23**:1522–1540. doi:10.1101/gr.156539.113
526 Zhang H, Lang Z, Zhu J-K. 2018. Dynamics and function of DNA methylation in plants. *Nature*
527   *Reviews Molecular Cell Biology* 1–1. doi:10.1038/s41580-018-0016-z
528 Zou L, Liu W, Zhang Z, Edwards EJ, Gathunga EK, Fan P, Duan W, Li S, Liang Z. 2020. Gene
529   body demethylation increases expression and is associated with self-pruning during grape
530   genome duplication. *Hortic Res* **7**:84. doi:10.1038/s41438-020-0303-7
531 Benaglia T, Chauveau D, Hunter DR, Young D. 2009. mixtools: An R Package for Analyzing Finite
532   Mixture Models. *Journal of Statistical Software* **32**:1–29.
533 Bender AT, Beavo JA. 2006. Cyclic Nucleotide Phosphodiesterases: Molecular Regulation to
534   Clinical Use. *Pharmacological Reviews* **58**:488–520. doi:10.1124/PR.58.3.5
535 Bernardi O, Bernardi D, Ribeiro RS, Okuma DM, Salmeron E, Fatoretto J, Medeiros FCL, Burd T,
536   Omoto C. 2015. Frequency of resistance to Vip3Aa20 toxin from Bacillus thuringiensis in
537   Spodoptera frugiperda (Lepidoptera: Noctuidae) populations in Brazil. *Crop Protection*
538   **76**:7–14. doi:10.1016/j.cropro.2015.06.006
539 Boaventura D, Buer B, Hamaekers N, Maiwald F, Nauen R. 2021. Toxicological and molecular
540   profiling of insecticide resistance in a Brazilian strain of fall armyworm resistant to Bt Cry1
541   proteins. *Pest Management Science* **77**:3713–3726. doi:10.1002/ps.6061
542 Boyko A, Blevins T, Yao Y, Golubov A, Bilichak A, Ilnytskyy Y, Hollander J, Meins F, Kovalchuk I.
543   2010. Transgenerational adaptation of Arabidopsis to stress requires DNA methylation and
544   the function of dicer-like proteins. *PLoS ONE* **5**. doi:10.1371/journal.pone.0009514
545 Brevik K, Bueno EM, McKay S, Schoville SD, Chen YH. 2021. Insecticide exposure affects
546   intergenerational patterns of DNA methylation in the Colorado potato beetle, Leptinotarsa
547   decemlineata. *Evolutionary Applications* **14**:746–757. doi:10.1111/eva.13153
548 Chakrabarty S, Jin M, Wu C, Chakraborty P, Xiao Y. 2020. Bacillus thuringiensis vegetative
549   insecticidal protein family Vip3A and mode of action against pest Lepidoptera. *Pest*
550   *Management Science* **76**:1612–1617. doi:10.1002/ps.5804
551 Chen P, Xiao WF, Pan MH, Xiao JS, Feng YJ, Dong ZQ, Zou BX, Zhou L, Zhang YH, Lu C. 2020.
552   Comparative genome-wide DNA methylation analysis reveals epigenomic differences in
553   response to heat-humidity stress in Bombyx mori. *International Journal of Biological*
554   *Macromolecules* **164**:3771–3779. doi:10.1016/j.ijbiomac.2020.08.251
555 Ding G, Cao L, Zhou J, Li Z, Lai Y, Liu K, Luo Y, Bai L, Wang X, Wang T, Wang R, Yang G, Sun
556   S. 2022. DNA Methylation Correlates with the Expression of Drought-Responsive Genes
557   and Drought Resistance in Rice. *Agronomy* **12**:1445. doi:10.3390/agronomy12061445
558 Dowen RH, Pelizzola M, Schmitz RJ, Lister R, Dowen JM, Nery JR, Dixon JE, Ecker JR. 2012.
559   Widespread dynamic DNA methylation in response to biotic stress. *Proceedings of the*
560   *National Academy of Sciences of the United States of America* **109**.
561   doi:10.1073/pnas.1209329109

562 Gao R, Li C-L, Tong X-L, Han M-J, Lu K-P, Liang S-B, Hu H, Luan Y, Zhang B-L, Liu Y-Y, Dai F-
563   Y. 2020. Identification, expression, and artificial selection of silkworm epigenetic
564   modification enzymes. *BMC Genomics* **21**:740. doi:10.1186/s12864-020-07155-z
565 Glastad KM, Hunt BG, Yi SV, Goodisman MAD. 2011. DNA methylation in insects: On the brink
566   of the epigenomic era. *Insect Molecular Biology* **20**:553–565. doi:10.1111/j.1365-
567   2583.2011.01092.x
568 Herb BR, Wolschin F, Hansen KD, Aryee MJ, Langmead B, Irizarry R, Amdam GV, Feinberg AP.
569   2012. Reversible switching between epigenetic states in honeybee behavioral subcastes. *Nat*
570   *Neurosci* **15**:1371–1373. doi:10.1038/nn.3218
571 Huang H, Wu P, Zhang S, Shang Q, Yin H, Hou Q, Zhong J, Guo X. 2019. DNA methylomes and
572   transcriptomes analysis reveal implication of host DNA methylation machinery in BmNPV
573   proliferation in Bombyx mori. *BMC Genomics* **20**. doi:10.1186/s12864-019-6146-7
574 Jansz N. 2019. DNA methylation dynamics at transposable elements in mammals. *Essays in*
575   *Biochemistry* **63**:677–689. doi:10.1042/EBC20190039
576 Jin M, Tao J, Li Q, Cheng Y, Sun X, Wu K, Xiao Y. 2021. Genome editing of the SfABCC2 gene
577   confers resistance to Cry1F toxin from Bacillus thuringiensis in Spodoptera frugiperda.
578   *Journal of Integrative Agriculture* **20**:815–820. doi:10.1016/S2095-3119(19)62772-3
579 Jjingo D, Conley AB, Yi SV, Lunyak VV, Jordan IK. 2012. On the presence and role of human
580   gene-body DNA methylation. *Oncotarget* **3**:462–474. doi:10.18632/oncotarget.497
581 Kou HP, Li Y, Song XX, Ou XF, Xing SC, Ma J, Von Wettstein D, Liu B. 2011. Heritable alteration
582   in DNA methylation induced by nitrogen-deficiency stress accompanies enhanced tolerance
583   by progenies to the stress in rice (Oryza sativa L.). *Journal of Plant Physiology* **168**:1685–
584   1693. doi:10.1016/j.jplph.2011.03.017
585 Lewis SH, Ross L, Bain SA, Pahita E, Smith SA, Cordaux R, Miska EA, Lenhard B, Jiggins FM,
586   Sarkies P. 2020. Widespread conservation and lineage-specific diversification of genome-
587   wide DNA methylation patterns across arthropods. *PLoS Genetics* **16**.
588   doi:10.1371/journal.pgen.1008864
589 Li B, Hu P, Zhu L-B, You L-L, Cao H-H, Wang J, Zhang S-Z, Liu M-H, Toufeeq S, Huang S-J, Xu
590   J-P. 2020. DNA Methylation Is Correlated with Gene Expression during Diapause
591   Termination of Early Embryonic Development in the Silkworm (Bombyx mori).
592   *International Journal of Molecular Sciences* **21**:671. doi:10.3390/ijms21020671
593 Li S, Peng Y, Panchenko AR. 2022. DNA methylation: Precise modulation of chromatin structure
594   and dynamics. *Current Opinion in Structural Biology* **75**:102430.
595   doi:10.1016/j.sbi.2022.102430
596 Li T, Liu N. 2017. Regulation of P450-mediated permethrin resistance in Culex quinquefasciatus by
597   the GPCR/Gαs/AC/cAMP/PKA signaling cascade. *Biochemistry and Biophysics Reports*
598   **12**:12–19. doi:10.1016/j.bbrep.2017.08.010
599 Lu K, Song Y, Zeng R. 2021. The role of cytochrome P450-mediated detoxification in insect
600   adaptation to xenobiotics. *Current Opinion in Insect Science* **43**:103–107.
601   doi:10.1016/j.cois.2020.11.004
602 Marshall H, Lonsdale ZN, Mallon EB. 2019. Methylation and gene expression differences between
603   reproductive and sterile bumblebee workers. *Evolution Letters* **3**:485–499.
604   doi:10.1002/evl3.129
605 Moore LD, Le T, Fan G. 2013. DNA methylation and its basic function.
606   *Neuropsychopharmacology: Official Publication of the American College of*
607   *Neuropsychopharmacology* **38**:23–38. doi:10.1038/npp.2012.112
608 Omar MAA, Li M, Liu F, He K, Qasim M, Xiao H, Jiang M, Li F. 2020. The Roles of DNA
609   Methyltransferases 1 (DNMT1) in Regulating Sexual Dimorphism in the Cotton Mealybug,
610   Phenacoccus solenopsis. *Insects* **11**:121. doi:10.3390/insects11020121

611 Palma L, Muñoz D, Berry C, Murillo J, Caballero P, Caballero P. 2014. Bacillus thuringiensis
612   toxins: An overview of their biocidal activity. *Toxins* **6**:3296–3325.
613   doi:10.3390/toxins6123296
614 Prodhomme C, Vos PG, Paulo MJ, Tammes JE, Visser RGF, Vossen JH, van Eck HJ. 2020.
615   Distribution of P1(D1) wart disease resistance in potato germplasm and GWAS
616   identification of haplotype-specific SNP markers. *Theoretical and Applied Genetics*
617   **133**:1859–1871. doi:10.1007/s00122-020-03559-3
618 Rajkumar MS, Gupta K, Khemka NK, Garg R, Jain M. 2020. DNA methylation reprogramming
619   during seed development and its functional relevance in seed size/weight determination in
620   chickpea. *Communications Biology* **3**. doi:10.1038/s42003-020-1059-1
621 Shaw S, Knüsel S, Abbühl D, Naguleswaran A, Etzensperger R, Benninger M, Roditi I. 2022.
622   Cyclic AMP signalling and glucose metabolism mediate pH taxis by African trypanosomes.
623   *Nature Communications* **13**:1–13. doi:10.1038/s41467-022-28293-w
624 Stassen JHM, López A, Jain R, Pascual-Pardo D, Luna E, Smith LM, Ton J. 2018. The relationship
625   between transgenerational acquired resistance and global DNA methylation in Arabidopsis.
626   *Scientific Reports* **8**. doi:10.1038/s41598-018-32448-5
627 Sun R-Z, Liu J, Wang Y-Y, Deng X. 2021. DNA methylation-mediated modulation of rapid
628   desiccation tolerance acquisition and dehydration stress memory in the resurrection plant
629   Boea hygrometrica. *PLOS Genetics* **17**:e1009549. doi:10.1371/journal.pgen.1009549
630 Uli N, Michelen-Gomez E, Ramos EI, Druley TE. 2018. Age-specific changes in genome-wide
631   methylation enrich for Foxa2 and estrogen receptor alpha binding sites. *PLOS ONE*
632   **13**:e0203147. doi:10.1371/journal.pone.0203147
633 Verhoeven KJF, Jansen JJ, van Dijk PJ, Biere A. 2010. Stress-induced DNA methylation changes
634   and their heritability in asexual dandelions. *New Phytologist* **185**:1108–1118.
635   doi:10.1111/j.1469-8137.2009.03121.x
636 Wang W, Huang F, Qin Q, Zhao X, Li Z, Fu B. 2015. Comparative analysis of DNA methylation
637   changes in two rice genotypes under salt stress and subsequent recovery. *Biochemical and
638   Biophysical Research Communications* **465**:790–796. doi:10.1016/j.bbrc.2015.08.089
639 Wang X, Li A, Wang W, Que H, Zhang G, Li L. 2021. DNA methylation mediates differentiation in
640   thermal responses of Pacific oyster (Crassostrea gigas) derived from different tidal levels.
641   *Heredity* **126**:10–22. doi:10.1038/s41437-020-0351-7
642 Wang X, Wheeler D, Avery A, Rago A, Choi J-H, Colbourne JK, Clark AG, Werren JH. 2013.
643   Function and Evolution of DNA Methylation in Nasonia vitripennis. *PLOS Genetics*
644   **9**:e1003872. doi:10.1371/journal.pgen.1003872
645 Watanabe H, Sugimoto R, Ikegami K, Enoki Y, Imafuku T, Fujimura R, Bi J, Nishida K, Sakaguchi
646   Y, Murata M, Maeda H, Hirata K, Jingami S, Ishima Y, Tanaka M, Matsushita K, Komaba
647   H, Fukagawa M, Otagiri M, Maruyama T. 2017. Parathyroid hormone contributes to the
648   down-regulation of cytochrome P450 3A through the cAMP/PI3K/PKC/PKA/NF-κB
649   signaling pathway in secondary hyperparathyroidism. *Biochemical Pharmacology* **145**:192–
650   201. doi:10.1016/j.bcp.2017.08.016
651 Wibowo A, Becker C, Marconi G, Durr J, Price J, Hagmann J, Papareddy R, Putra H, Kageyama J,
652   Becker J, Weigel D, Gutierrez-Marcos J. 2016. Hyperosmotic stress memory in Arabidopsis
653   is mediated by distinct epigenetically labile sites in the genome and is restricted in the male
654   germline by DNA glycosylase activity. *Elife* **5**:e13546. doi:10.7554/eLife.13546
655 Xiao Y, Wu K. 2019. Recent progress on the interaction between insects and Bacillus thuringiensis
656   crops. *Philosophical Transactions of the Royal Society B: Biological Sciences* **374**.
657   doi:10.1098/rstb.2018.0316
658 Xu G, Lyu H, Yi Y, Peng Y, Feng Q, Song Q, Gong C, Peng X, Palli SR, Zheng S. 2021. Intragenic
659   DNA methylation regulates insect gene expression and reproduction through the
660   MBD/Tip60 complex. *iScience* **24**:102040. doi:10.1016/j.isci.2021.102040

Xu G, Lyu J, Li Q, Liu H, Wang D, Zhang M, Springer NM, Ross-Ibarra J, Yang J. 2020. Evolutionary and functional genomics of DNA methylation in maize domestication and improvement. *Nature Communications* **11**. doi:10.1038/s41467-020-19333-4

Yang F, Kerns DL, Little NS, Santiago González JC, Tabashnik BE. 2021a. Early Warning of Resistance to Bt Toxin Vip3Aa in Helicoverpa zea. *Toxins (Basel)* **13**:618. doi:10.3390/toxins13090618

Yang F, Williams J, Huang F, Kerns DL. 2021b. Genetic basis and cross-resistance of Vip3Aa resistance in Spodoptera frugiperda (lepidoptera: Noctuidae) derived from Texas, USA. *Crop Protection* **147**:105702. doi:10.1016/j.cropro.2021.105702

Yang F, Williams J, Porter P, Huang F, Kerns DL. 2019. F2 screen for resistance to Bacillus thuringiensis Vip3Aa51 protein in field populations of Spodoptera frugiperda (Lepidoptera: Noctuidae) from Texas, USA. *Crop Protection* **126**:104915. doi:10.1016/j.cropro.2019.104915

Yang X, Chen W, Song X, Ma X, Cotto-Rivera RO, Kain W, Chu H, Chen YR, Fei Z, Wang P. 2019. Mutation of ABC transporter ABCA2 confers resistance to Bt toxin Cry2Ab in Trichoplusia ni. *Insect Biochemistry and Molecular Biology* **112**:103209. doi:10.1016/j.ibmb.2019.103209

Yang X, Han H, DeCarvalho DD, Lay FD, Jones PA, Liang G. 2014. Gene body methylation can alter gene expression and is a therapeutic target in cancer. *Cancer Cell* **26**:577–590. doi:10.1016/j.ccr.2014.07.028

Yu G, Wang LG, Han Y, He QY. 2012. ClusterProfiler: An R package for comparing biological themes among gene clusters. *OMICS A Journal of Integrative Biology* **16**:284–287. doi:10.1089/omi.2011.0118

Zemach A, McDaniel IE, Silva P, Zilberman D. 2010. Genome-wide evolutionary analysis of eukaryotic DNA methylation. *Science* **328**:916–919. doi:10.1126/science.1186366

Zhang Bo, Zhou Y, Lin N, Lowdon RF, Hong C, Nagarajan RP, Cheng JB, Li D, Stevens M, Lee HJ, Xing X, Zhou J, Sundaram V, Elliott G, Gu J, Shi T, Gascard P, Sigaroudinia M, Tlsty TD, Kadlecek T, Weiss A, O'Geen H, Farnham PJ, Maire CL, Ligon KL, Madden PAF, Tam A, Moore R, Hirst M, Marra MA, Zhang Baoxue, Costello JF, Wang T. 2013. Functional DNA methylation differences between tissues, cell types, and across individuals discovered using the M&M algorithm. *Genome Res* **23**:1522–1540. doi:10.1101/gr.156539.113

Zhang H, Lang Z, Zhu J-K. 2018. Dynamics and function of DNA methylation in plants. *Nature Reviews Molecular Cell Biology* 1–1. doi:10.1038/s41580-018-0016-z

Zou L, Liu W, Zhang Z, Edwards EJ, Gathunga EK, Fan P, Duan W, Li S, Liang Z. 2020. Gene body demethylation increases expression and is associated with self-pruning during grape genome duplication. *Hortic Res* **7**:84. doi:10.1038/s41438-020-0303-7

Author contributions:

Conceptualization: LZ, YX

Methodology: LZ, MJ, ZL

Investigation: LZ, MJ, ZL, YS

Visualization: LZ

Supervision: YX

Writing—original draft: LZ

Writing—review & editing: LZ, PW, YX

Competing interests

The authors declare that they have no competing interests.

Materials availability

All the materials used in the study are available upon reasonable request from the corresponding author.

Data Accessibility Statement

All the Oxford nanopore technique and RNA sequencing data are available from NCBI Sequence Read Archive (SRA) database with accession number PRJNA938165. Metadata are also stored in the SRA (PRJNA938165) in TSV format.

721
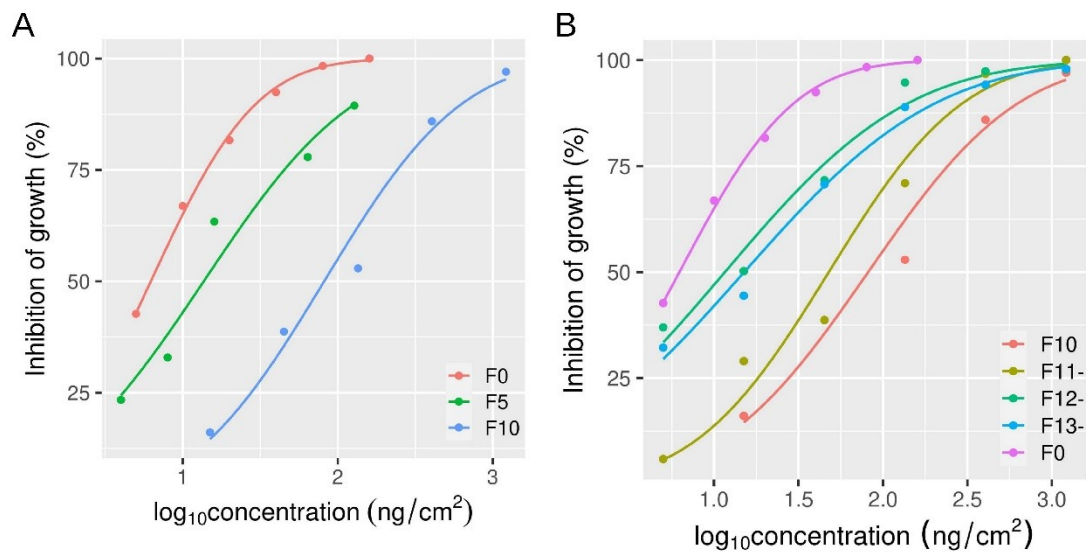
Fig. 1. Inhibition curves of Vip3Aa on Vip3Aa screened fall armyworm (FAW). (A) Inhibition
curves of original generation (F0) and the generations screened by Vip3Aa for five (F5) and ten
(F10) generations. **(B)** Inhibition curves of F0, Vip3Aa screened tenth generation (F10+) and its
next three progenies that were cultivated without Vip3Aa (F11-, F12-, and F13-).

726
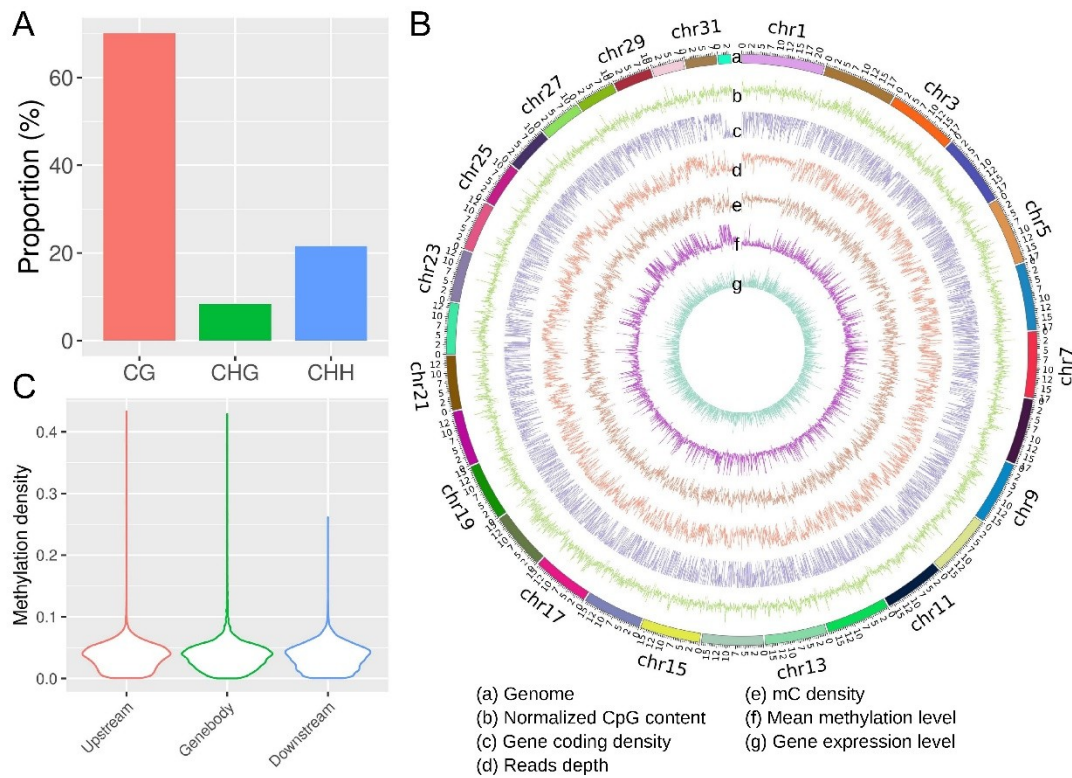
Fig. 2. Integration of genome, methylome, and transcriptome. (A) Methylated context

proportions. **(B)** Circos plot that shows the (b) normalized CpG content, (c) gene coding density, (d)

mean sequencing depth, (e) methylcytosine (mC) density, (f) mean methylation level, and (g)

normalized *tags* per kilobase *per million mapped reads* value in the 50 kb level. **(C)** Distribution of

mC densities of upstream, gene body, and downstream.

734
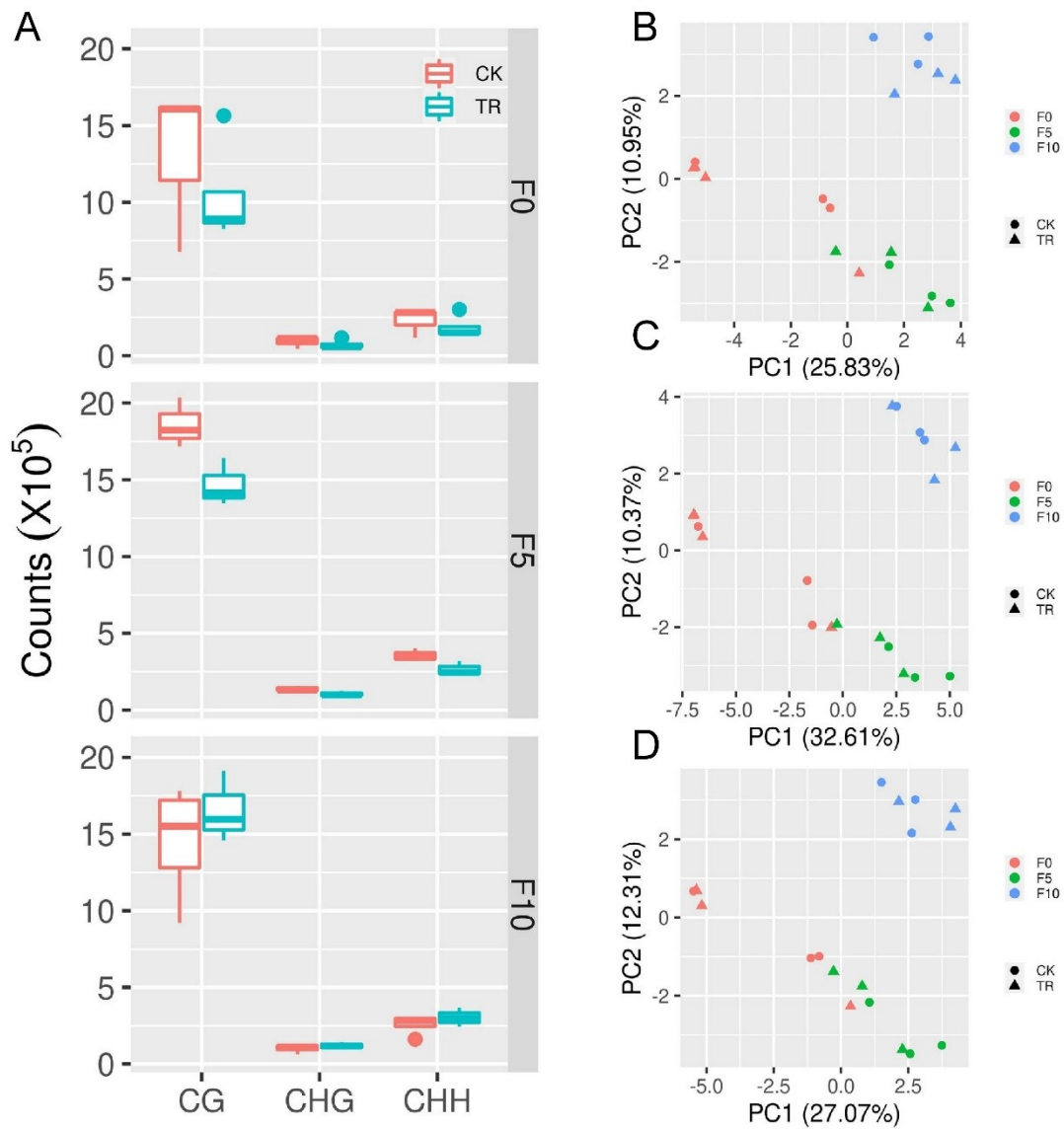
Fig. 3. Methylated context counts and principal components analysis of gene region methylcytosine densities. (A) Methylated context counts in F0, F5, and F10 controls and their Vip3Aa treatments. PCA of **(B)** upstream, **(C)** genebody, and **(D)** downstream mC densities for each sample.

739

740
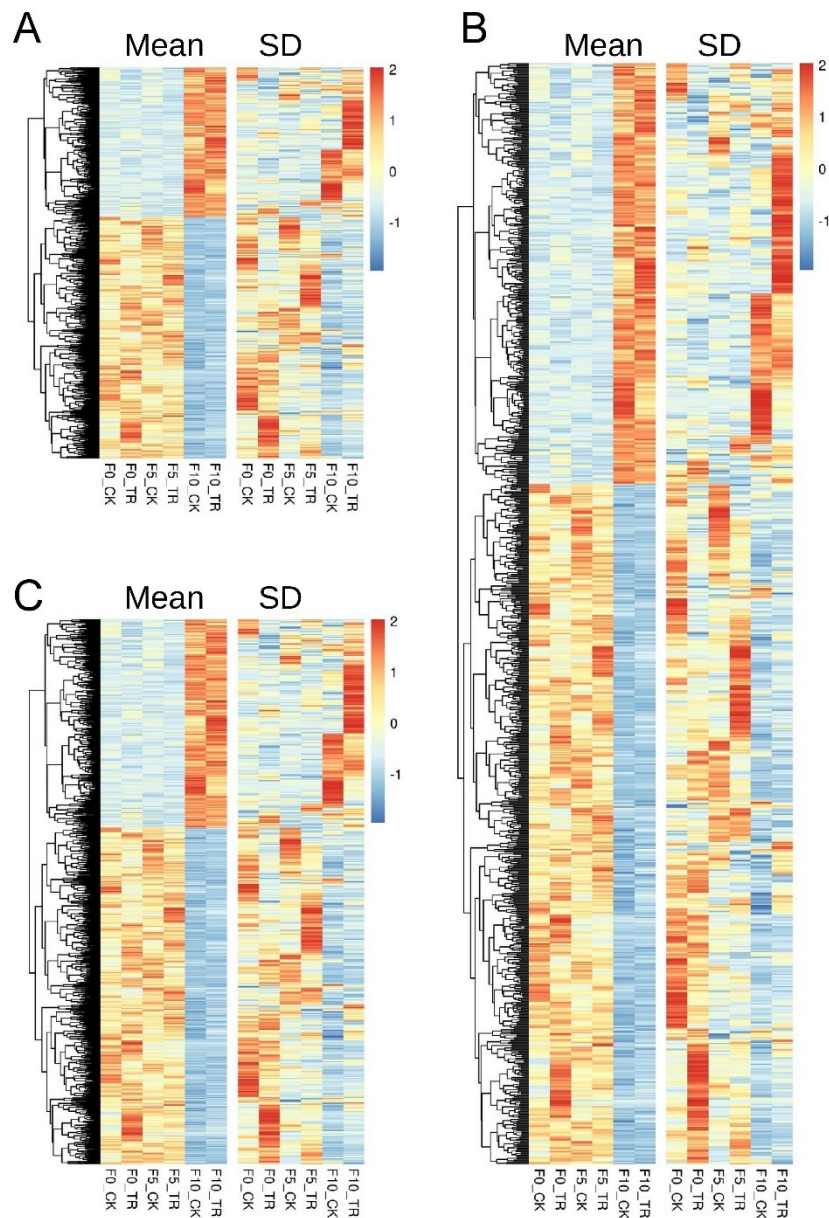
Fig. 4. Mean and standard error patterns of methylcytosine (mC) densities for differentially methylated genes. Patterns of mean and standard errors ($n = 3$) of the **(A)** upstream, **(B)** genebody, and **(C)** downstream mC densities for differentially methylated genes. F0, F5, and F10 represent the original, fifth, and tenth generation, respectively. CK and TR represent the control and Vip3Aa-treated groups.

746
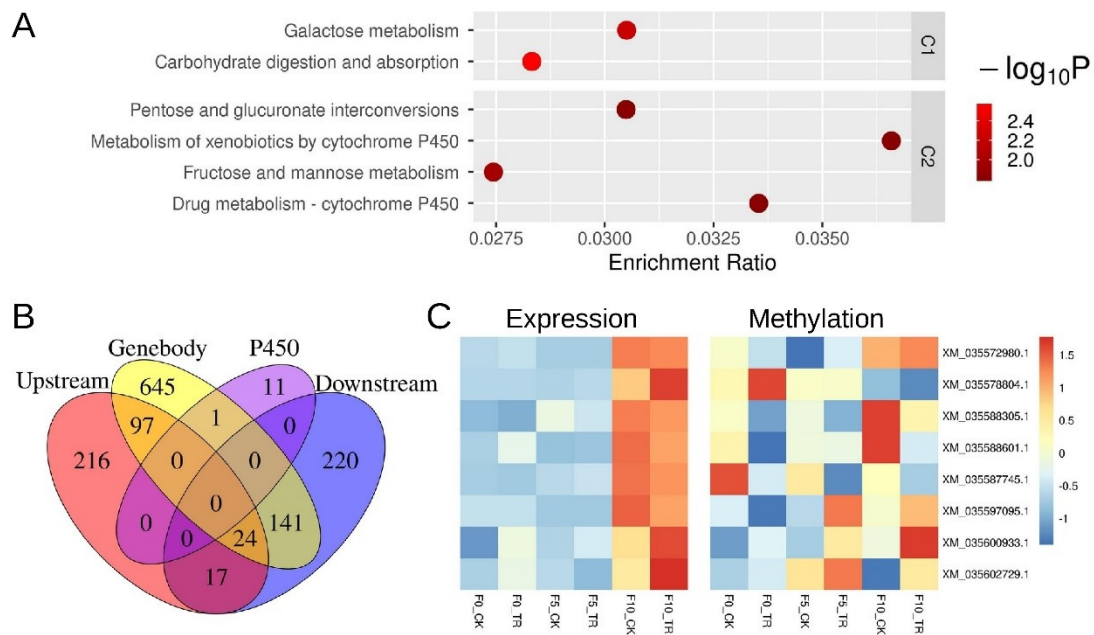
Fig. 5. KEGG enrichment of Vip3Aa resistance positively correlated differentially expressed gene cluster. (A) Significantly enriched KEGG pathways in resistance positively correlated differentially expressed gene cluster (P_{fdr} < 0.05). **(B)** Relationship between significantly enriched P450 genes and differentially methylated genes. **(C)** Expression levels and gene body methylation density patterns of significantly enriched P450 genes.

754
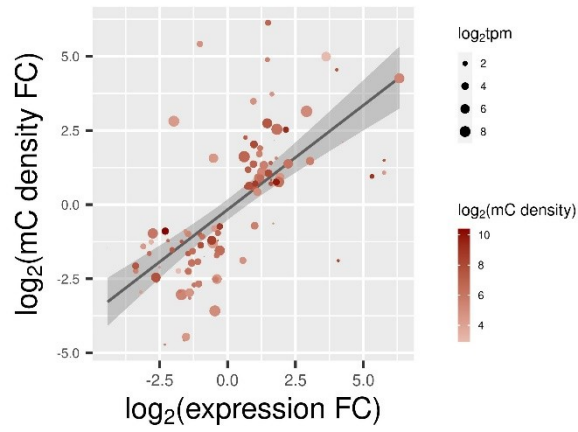
Fig. 6. Point plot of the differentially expressed and methylated genes in the gene body based on the comparison log2 fold change between F10 and F0 control groups. The line was produced by loess analysis, and the dark grey area represents 95% confidence interval. The size and color of each point represent the maximum values for the log2 transformation of mythylcytosine densities and TPM in F10 or F0 control groups for each gene, receptively.

760

761
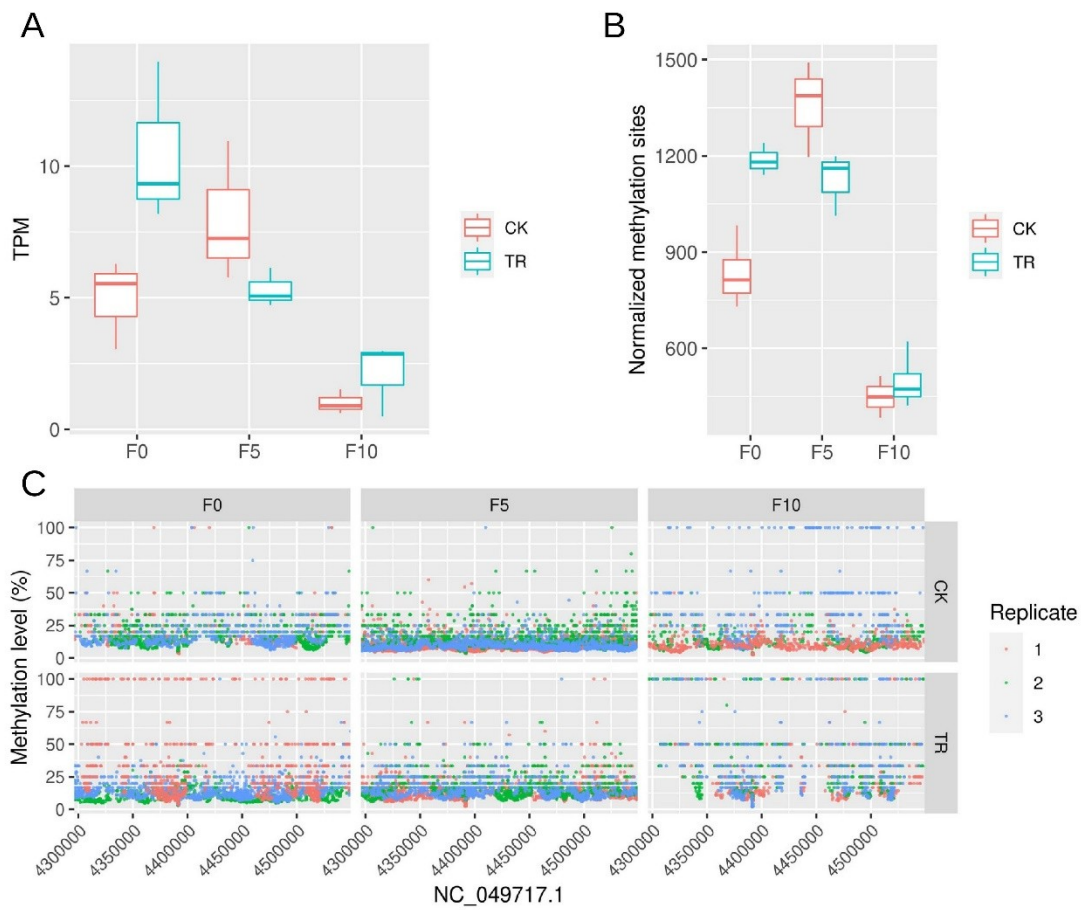
Fig 7 Expression levels and methylation status of fall armyworm mid-gut *SfPDE8A* gene under
normal diet (CK) and Vip3Aa diet (TR). (A) Mean TPM. (B) Boxplot of normalized methylcytosine
numbers. (C) Methylation status of *SfPDE8A* gene region. F0, F5, and F10 represent the original,
the fifth, and the tenth generation, respectively.

766

767
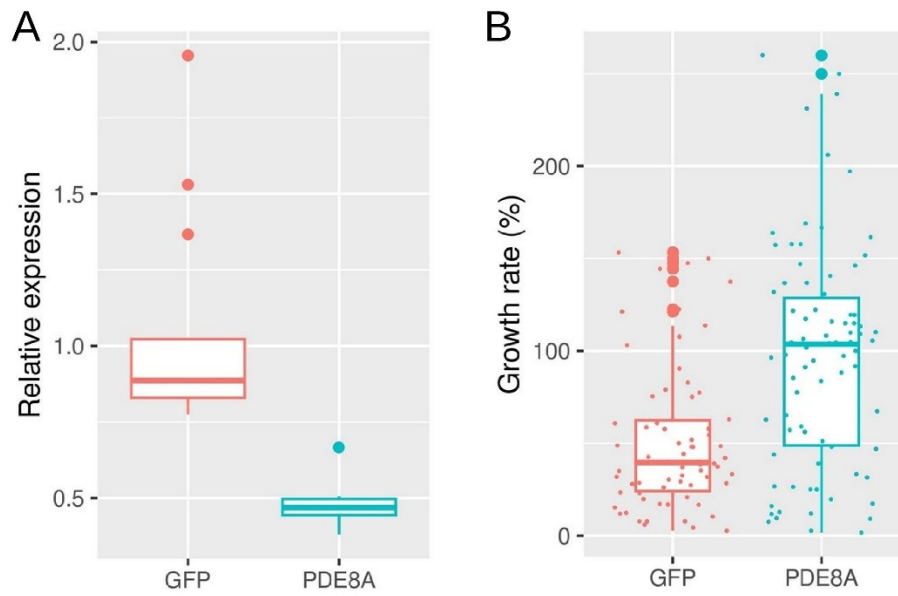
Fig 8 *SfPDE8A* gene knock-down significantly increased fall armyworm (FAW) Vip3Aa resistance.
(A) Growth rate of FAW third-instar larvae injected with GFP and *SfPDE8A* dsRNAs after 72 h. (B)
Relative expression levels of *SfPDE8A* in the third-instar FAW larval mid-gut 72 h after GFP and
SfPDE8A dsRNA injection.

772

773

774 **Supplementary Materials**

775   Include:

776   Fig. S1 to S19.

777   Table S1 and S2.

778